RESEARCH ARTICLE | NOVEMBER 12 2021

Quasi-steady testing approach for high-power Hall thrusters

Special Collection: Physics of Electric Propulsion

Lubos Brieda ; Yevgeny Raitses ; Edgar Choueiri; Roger Myers; Michael Keidar

Journal of Applied Physics 130, 183303 (2021)
https://doi.org/10.1063/5.0067232

Journal of Applied Physics ARTICLE scitation.org/journal/jap

Quasi-steady testing approach for high-power Hall thrusters

Cite as: J. Appl. Phys. **130**, 183303 (2021); doi: 10.1063/5.0067232
Submitted: 15 August 2021 · Accepted: 6 October 2021 ·
Published Online: 12 November 2021

View Online Export Citation CrossMark

Lubos Brieda,[1,a)] Yevgeny Raitses,[2] Edgar Choueiri,[3] Roger Myers,[4] and Michael Keidar[5]

AFFILIATIONS

[1]Particle In Cell Consulting LLC, Westlake Village, California 91362, USA
[2]Princeton Plasma Physics Laboratory, Princeton, New Jersey 08543, USA
[3]Electric Propulsion and Plasma Dynamics Laboratory, Princeton University, Princeton, New Jersey 08544, USA
[4]R. Myers Consulting LLC, Woodinville, Washington 98072, USA
[5]Department of Mechanical and Aerospace Engineering, The George Washington University, Washington, DC 20052, USA

Note: This paper is part of the Special Topic on Physics of Electric Propulsion.
[a)]**Author to whom correspondence should be addressed:** lubos.brieda@particleincell.com

ABSTRACT

Hall effect thrusters operating at power levels in excess of several hundreds of kilowatts have been identified as enabling technologies for applications such as lunar tugs, large satellite orbital transfer vehicles, and solar system exploration. These large thrusters introduce significant testing challenges due to the propellant flow rate exceeding the pumping speed available in most laboratories. Even with proposed upgrades in mind, the likelihood that multiple vacuum facilities will exist in the near future to allow long duration testing of high-power Hall thrusters operating at power levels in excess of 100 kW remains extremely low. In this article, we numerically explore the feasibility of testing Hall thrusters in a quasi-steady mode defined by pulsing the mass flow rate between a nominal and a low value. Our simulations indicate that sub-second durations available before the chamber reaches critical pressure are sufficiently long to achieve the steady-state current and flow field distributions, allowing us to characterize thruster performance and the near plume region.

I. INTRODUCTION

Hall effect thrusters (HETs) are spacecraft electric propulsion (EP) devices routinely used for orbit raising, repositioning, and solar system exploration applications. To date, the highest power Hall thruster flown is the 4.5 kW BPT-4000 launched in 2010 aboard the Advanced EHF satellite[1] (which the HET helped to deliver to the correct orbit after a failure of the primary chemical booster), although a 13 kW system is being readied for near-term flight operation as part of the Lunar Gateway,[2] and thrusters at 50[3,4]–100 kW[s] power levels have been demonstrated in the laboratory. Solar cell advancements and a renewed interest in nuclear power has led the aerospace community to consider the use of Hall thrusters operating at even higher power levels. Multi-hundred kW EP systems would offer an economical solution for LEO to GEO orbit raising or for deployment of a Earth-to-Moon delivery tug, and power levels in excess of 600 kW could be utilized for crewed transport to Mars.[5–9] While such power levels could be delivered using existing devices, a single large thruster requires less system mass and has a reduced footprint than a cluster of smaller devices.[10]

At these high power levels, it becomes difficult, if not outright impossible, for vacuum chamber pumps to keep up with the propellant mass injection rates. Numerous experiments have found Hall thruster performance to be influenced by the ground facility effects. While the vacuum chamber also introduces new electrical current pathways,[11,12] the primary contributing factor is the chamber pressure. Thrust is observed to vary almost linearly with increasing background pressure, suggesting that a return flux of wall-neutralized beam ions acts as an additional propellant source.[13] For the NASA 173M thruster (operating in the power range of 1.5–4.0 kW), thrust was observed to vary by about 3% over the typical pressure ranges encountered in ground testing,[14] while for other models, variations approaching 10% have been reported. The background pressure also affects beam divergence[15] and cathode coupling, especially with non-centrally mounted cathodes,[16] leading to the acceleration zone moving upstream,[7] and thus altering the voltage drop through which the propellant is accelerated. The frequency of discharge oscillations is also affected, although this response does not seem to be universal. In the Princeton cylindrical HET (operating in the range of 50–300 W), breathing mode frequency and amplitude remained mainly constant until about 5×10^{-5} Torr after which they disappeared.[17] Note that we utilize the non-SI unit of Torr (1 Torr $\approx$ 133.32 Pa; 5×10^{-5} Torr $\approx 6.67 \times 10^{-3}$ Pa) due to its prevalence in the field of electric propulsion vacuum testing. The rotating spoke increased in frequency until this pressure after which it also disappeared. Matlock *et al.*[18] considered pressure effects in a different 1 kW PPPL thruster and found it to exhibit a strong frequency dependence on background pressure for both the anode current or cathode potential waveforms. Overall, these varied ground facility impacts, including sometimes conflicting results, call into question whether ground testing properly simulates in-space operation and highlight the fact that the challenge will become much harder as thruster power increases.

The early work on pressure effects of Randolph *et al.* has suggested that HETs should be tested below 5×10^{-5} Torr.[19] However, even this level may not be sufficiently conservative, given that thrust is observed to continue decreasing further as the pressure is lowered without an apparent asymptotic plateau.[20] In fact, the SPT-100 thruster was found to be the most sensitive to variations at $\approx 3 \times 10^{-5}$ Torr.[21] Yet, a recent survey of international facilities found that the vast majority of existing chambers are simply unable to maintain pressures in the 10^{-5} Torr range when used with 100 kW devices.[10,22] To the best of our knowledge, there are no facilities anywhere that can maintain this pressure with a 1 MW Hall thruster. Some facilities may be able to run a pod of 100 kW thrusters, but the thrusters must be in a close proximity leading to a large number of unknowns in the plume-to-plume interaction. Clearly, such a limited testing capacity drastically limits the development of high-power devices by placing research well beyond the capabilities of university and small business programs. In fact, testing of the 100 kW Nested Hall thruster (NHT) at University of Michigan had to be reduced to only a partial operation at 30 kW due to facility limitations,[7] despite access to one of the largest academic electric propulsion testing facilities in the United States. The full scale testing had to be delayed until Vacuum Facility 5 (VF-5) at the NASA Glenn Research Center became available. This chamber, measuring 15 ft in diameter and 60 ft in length, recently underwent an extensive simulation-driven retrofit[23,24] to help achieve its theoretical maximum pumping speed of 3.5×10^{6} l/s on air thanks to 6 cryopumps and 20 oil diffusion pumps. The facility at the Aerospace Corporation also recently underwent a redesign to increase pumping capabilities in support of anticipated future high-power EP testing campaign.[25] Yet even this second high-power facility is not expected to be sufficient given the rapid increase in the use of EP. The facilities can be envisioned to be occupied by months-long wear testing campaigns,[26] adversely affecting the development of new devices.

To address the pressure effect issues, some researchers have considered the use of metal or liquid propellants that condense on the facility walls.[27] Such propellants pose contamination risk to spacecraft and thus may be of limited practical use. In this article, we carry out a numerical study to assess the feasibility of an alternate scheme based on a quasi-steady pulsed operation. In order to reduce start-up transients, we assume that all thruster operating conditions, including the magnet current and cathode–anode coupling potential, remain in the nominal configuration. The only variation is the reduction in the anode propellant flow rate by two orders of magnitude to allow the chamber pressure to decay. The reduced mass flow is utilized in order to maintain a low density discharge to aid with reignition. It should be noted that this is not a completely novel idea. The quasi-steady pulsed approach has been utilized for decades at Princeton University[28,29] and at NASA Glenn VF-1 and VF-5 facilities,[30] as an economical option for VASIMR and MW-class MPD thruster research and testing. Pulsed mode has also been suggested for on-orbit operation to deliver fine propulsive bits.[31,32] We utilize the industry standard HET simulation code HPHall[33] to perform a series of simulations based on the 1.35 kW SPT-100 thruster placed in a scaled down chamber with a limited pumping capacity. This route was selected after an initial effort of scaling up the SPT-100 simulation to a MW class proved challenging. We begin the article by reviewing a 0D model for estimating chamber pressure variation. Subsequently, we describing the modifications made to HPHall and present results from the numerical study.

II. CYCLED OPERATION

From mass conservation, the temporal evolution of chamber pressure is governed by the balance between the injected and the removed mass, with the latter typically specified in terms of pumping speed. This volumetric quantity is related to the mass flow through the gas mass density. Here we neglect transient effects such as the flash-off of surface-adhered water on initial activation or the decay in composite outgassing rates and simply assume a constant baseline pressure. We also ignore the transit time associated with the finite molecular speed (which for xenon is approximately 220 m/s at room temperature) and treat the pumping speed as a constant with respect to chamber pressure. We also ignore finite conductance reduction introduced by the geometrical configuration of the chamber. From the ideal gas law at constant temperature, we have

$$\frac{\partial p}{\partial t} = \frac{\partial n}{\partial t} k_B T. \tag{1}$$

Considering the entire vacuum chamber as a single control volume, mass conservation yields

$$\frac{\partial n}{\partial t} = \frac{1}{mV}\left(\dot{m}_{in} - \dot{m}_{pump}\right). \tag{2}$$

The rate of mass removal is given by $\dot{m}_{pump} = \rho S$, where S is the pumping speed. Power of an EP device can be related to the mass flow rate with

$$P = \eta V \dot{m}_{in} Z_i e/m, \tag{3}$$

where η is the efficiency, V is the discharge voltage, $\dot{m}_{in}$ is the injected mass flow rate, Z_i is the mean ion ionization state, e is the elementary charge, and m is the working gas atomic mass. Numerical integration of Eq. (1) with dimensions of the University of Michigan Large Vacuum Facility and pumping speed of 240 000 l/s on xenon[s] leads to the plot in Fig. 1. This facility was chosen as an example of a large chamber that may be available at university settings. Here we used $\eta = 0.9$, $V = 300\,\text{V}$, and $Z_i = 1.1$. We also considered four different power levels ranging from 1 kW to 1 MW and set the baseline pressure to 10^{-7} Torr. The thruster was assumed to operate for 30 s in the nominal mode. The injection flow rate is then reduced by a factor of 100. This low-flow mode is envisioned to help maintain a low-density plasma population to aid with reignition. The mass flow rate is subsequently returned to the nominal level to demonstrate repeatability.

In all configurations, we observe the chamber pressure first rising rapidly but then stabilizing within approximately 15 s. Next, we also observe a decrease in pressure once the flow rate is reduced, with the chamber stabilizing at a new baseline within 30 s. It should be noted that in the real chamber, both of these time periods would be extended by the molecular transit time and non-constant pumping speeds, which are here ignored. Switching back to the nominal flow rate returns the pressure to the level observed on the first cycle. This sequence can be repeated for as long as needed, with occasional breaks for cryopanel regeneration.

For the 1 and 10 kW thrusters, the pressure remains below 5×10^{-5} Torr level at all times, thus confirming the experimental heritage of using similar facilities for testing at these power levels. At 100 kW and 1 MW, this threshold is breached after 1.08 and 0.050 s, respectively. The initial pressure rise, before the 5×10^{-5} Torr level is reached, may thus be used to obtain performance data free from facility pressure effects. While these time periods may appear short, they are sufficiently long in the frame of reference of Hall thruster dynamics. Even the 50 ms interval corresponds to 750 breathing mode cycles at a 15 kHz frequency. As demonstrated by Sekerak and Lobbia, modern high speed plasma probes can resolve plume properties at 5 μs intervals,[34,35] offering us 10 000 unique measurements within this window. The actuation of probes to the next sampling location would be done during the low-flow cycle, and thus, the cycled operation should have a minimal impact on the total duration of a plume mapping campaign. Fast electromagnetic valves with delay times shorter than 40 μs and a 160 μs pulse full width at half maximum have been developed in support of pulsed inductive plasma thrusters as reported by Guo.[36] These valves were demonstrated to deliver up to 2.5 mg of argon gas per pulse, which translates to mass flow rates in excess of those required even for a 1 MW class Hall thruster.

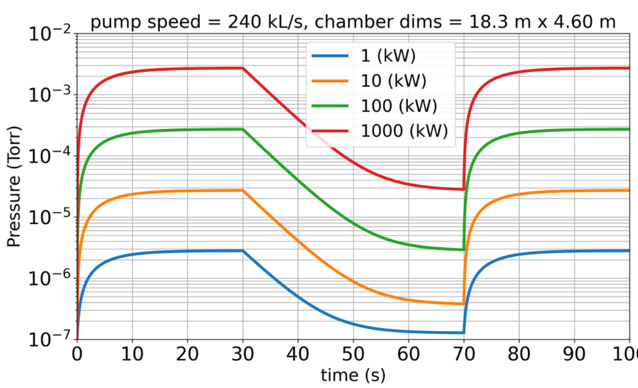

FIG. 1. Temporal evolution of chamber pressure assuming nominal operation for 30 s followed by a 40 s interval with flow rate reduced 100×. The colors correspond to 1 kW, 10 kW, 100 kW, and 1 MW power levels. The process is then repeated.

A significant unknown is a quantification of the start-up behavior during a pulsed operation. Hall thrusters are known to exhibit a current spike when they are first operated after a chamber pump down. Despite the limited available literature, it does not appear that this spike is present on subsequent restarts. For example, while Hargus[37] found the initial anode current transient to last for 300–500 s, this behavior was not observed on subsequent restarts after the thruster had been conditioned. The current transient would reappear after the chamber has been opened to the atmosphere or after cryopanels have been regenerated, which exposed the thruster to a "dirty" vacuum, characterized by the presence of water vapor and volatile gases. A typical regeneration cycle involves valving off the cryopump from the chamber and utilizing a downstream rough vacuum pump to remove the material evaporated from the warmed up panels. An oil-based pump could introduce volatile contaminant gases into the pump cavity, which can subsequently diffuse into the main chamber upon the completion of the regen cycle. It is also well known that a thin film of water forms on surfaces (and inside porous materials) exposed to atmosphere and boils off upon exposure to vacuum. Surface water concentration is also increased by the ambient air reaching dew point during pump down as the temperature decreases with the pressure. A subsequent study utilized a residual gas analyzer (RGA) and indeed found that hydrogen emission profiles follow the anode spike closely, further reinforcing the hypothesis that the excess anode current during the start transient is due to water vapor release[38] and, as such, should not reappear during pulsing. Another experimental study by Santos[39] looked at the startup process using a Princeton thruster and found that the transitional regime is characterized by a 20% increase in the discharge current for 15–30 min. This study correlated the presence of gas impurities such as water, hydrogen, or nitrogen with the increase in discharge current. The porous boron nitride used to line channel walls was identified as one possible source of the contaminants.

Therefore, once the thruster is conditioned and contaminants have been depleted, we can expect the ignition to be governed by the fluid and electrodynamic transient times. Fast camera imaging has demonstrated that Hall thrusters settle into steady-state operation with about 50 μs.[40,41] This is further evidenced by ignition videos that demonstrate an essentially instantaneous steady plume formation.[42,43] Busek analytical and experimental study demonstrated that for the BHT-200 thruster, the startup electrical transients decay within 0.06 ms and the peak discharge current is reached within 0.2 ms. The time required to fill the discharge channel with neutrals was around 10 ms. The longest identified transient effect was associated with the diffusion of the magnetic field throughout the discharge, which was observed to take about 20 ms. This effect may not be relevant to our proposed quasi-steady testing approach given that the discharge is never completely shut off. Based on this analysis and experimental observations, the authors estimated the minimum pulse required to achieve 80% of the steady-state performance to be between 30 and 50 ms.[31] This is comparable to the pressure rise time for the 1 MW thruster as seen in Fig. 1.

III. NUMERICAL SIMULATIONS

We next used the popular Hall thruster modeling tool HPHall to simulate a thruster operating in the quasi-steady mode. This code was originally developed by Fife at MIT[33] and has since been upgraded by a number of other researchers.[44–47] HPHall uses simulation particles to represent the heavy neutral and ion species using the Particle-in-Cell (PIC) method. The electron population is treated as a fluid with motion decoupled into the direction parallel and perpendicular to the magnetic field lines. Electrons are free to move along a field line, allowing one to write a relationship relating the local potential to a reference "thermalized" potential ϕ^* and the local density, $\phi = \phi^* + (kT_e/e)\ln(n_e)$. In the perpendicular direction, current balance $I_a = I_i + I_e + I_w$ is used to derive an expression for the variation of ϕ^* with the magnetic field line temperature, $T(\lambda)$. HPHall is thus predominantly an electron temperature solver for the following form of the energy equation:

$$\frac{\partial}{\partial t}\left(\frac{3}{2}n_e k T_e\right) + \nabla\cdot\left(\frac{5}{2}n_e k T_e \vec{u}_e + \vec{q}_e\right) = S_h - S_i, \tag{4}$$

where $S_h = \vec{j}_e \cdot \vec{E}$ and $S_i = \dot{n}_e \varphi' E_i$ are energy sources due to Ohmic heating and inelastic losses associated with ionization and the u_e is the velocity term obtained from Ohm's law. The computed temperature is used to set ϕ^* and the corresponding 2D potential that is then used in the PIC method to set the electric field that accelerates the ions. Electron temperature is also used to compute the ionization rate. HPHall has been applied to numerous thrusters; however, the Russian-developed SPT-100 is regularly used for benchmarking due to a ready availability of the magnetic field. In this work, we have utilized the same simulation inputs as in a prior work focusing on electrical coupling.[48] The nominal mass flow rate was set to $\dot{m} = 5.01 \times 10^{-6}$ kg/s. Simulation time step was set to $\Delta t = 10^{-7}$ s, with the code run for up to 10×10^6 time steps. The cathode line serves as a Dirichlet boundary for the electron energy solver and was set to $T_{e,cathode} = 3.5$ eV throughout the simulation. We also assumed that the power supply maintains a 300 V discharge voltage with cathode to ground coupling potential held at −20 V. It is feasible that cathode properties will be affected by the variation in plume density during the low-flow mode, but this quantification remains as future work.

A. Chamber neutral injection model

Fife's legacy HPHall allowed setting a scalar background density that was added to the spatially varying value computed from the particles. Parra subsequently introduced the ability to use the downstream boundary as an injection source of constant flux neutral particles. This kinetic approach allowed approximating the backstreaming found in a vacuum facility. The flux for each "panel" (a radially revolved cell edge) is computed from

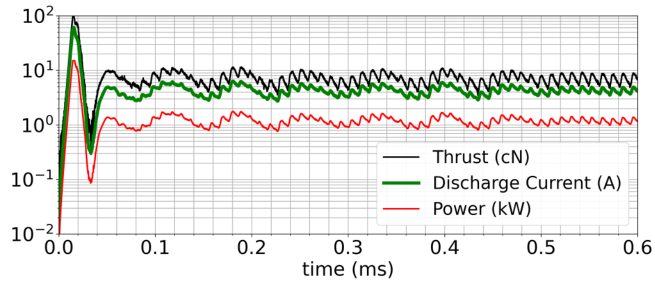

FIG. 2. Temporal evolution of discharge parameters at nominal configuration.

$$\Gamma = p\frac{mk_B}{T}\sqrt{\frac{k_B T}{2\pi m}}. \tag{5}$$

The code loops over the downstream panels and on each generates a user-specified number of neutral macroparticles with simulation weight set according to the injection flux and the revolved panel area. The neutral velocity is set to $v_n = \sqrt{8k_B T/(\pi m)}$ and an isotropic velocity is sampled such that $\vec{v}\cdot\hat{n} > 0$, where $\hat{n}$ is the panel normal vector pointing into the computational domain.

This algorithm was modified to dynamically update the chamber pressure used in Eq. (5) according to the provided chamber volume and pumping speed. Pump mass collection rate is first computed per $\dot{m}_{pump} = \rho S$, where $\rho = m_i p/(k_B T)$ assumes uniform pressure distribution and m_i is the molecular mass of the ion species. The pressure rate of change is then computed per Eq. (1), with $\dot{n}$ obtained from

$$\dot{n} = (\dot{m}_{thruster} - \dot{m}_{pump})/(V_{chamber} m_i). \tag{6}$$

We also add the option to include a fixed $\dot{p}$ term to model the constant rate of pressure increase effects. The chamber pressure is updated

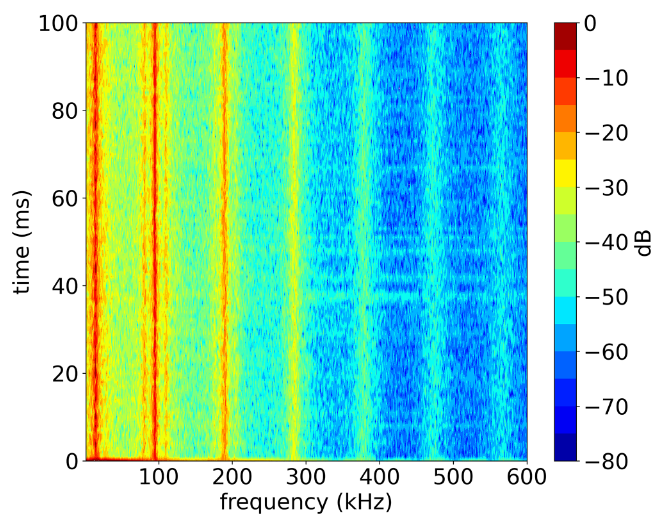

FIG. 3. Frequency power spectrum for the nominal configuration.

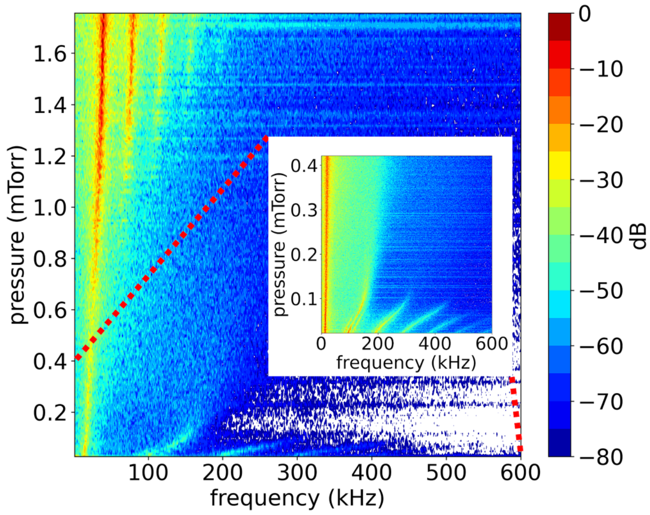

FIG. 4. Discharge current frequency spectrum for a linear 10^{-2} (10^{-3} inset) Torr/s pressure increase.

with the Forward Euler method, $p^{k+1} = p^k + (\dot{p}^k + \dot{p}^k_{fixed})\Delta t$. The relevant facility properties are specified in the input parm.in file.

B. Quasi-steady simulations

HPHall was also modified to support a quasi-steady mode operation. The injection mass flow rate is one of the many parameters listed in the input file. In addition to this $\dot{m}$ value, we now also load values for $\dot{m}_{low}$, and $t_{pulse,nom}$ and $t_{pulse,low}$. These intervals, if specified, turn on the quasi-steady operation in which the thruster alternates between the nominal and the low mass flow rate modes. The transition was assumed to be instantaneous.

IV. SIMULATION RESULTS

A. Nominal operation

Figure 2 plots the temporal evolution of the simulated discharge current, thrust, and power ($P = IV$) from a nominal operation with constant background pressure and time-invariant propellant flow rate. The simulation was started by first running in a neutrals-only mode to fill the discharge channel with the neutral propellant. The code was then restarted in the normal mode, which would be analogous to turning on the power supply to force ignition. The plot shows data only from this "normal" mode run. Despite not directly modeling outgassing or magnetic field ramp up, it is interesting to observe that the numerical simulation predicts a current spike similar to experimental observations. The discharge stabilizes within 0.05 ms, in agreement with the electrical transient measurements reported in Ref. 31 and fast camera imaging in Ref. 39. The magnetic field is applied externally, and as such, this simulation would not capture any transient effects associated with energization of the magnetic circuits. The thruster subsequently establishes the oscillatory steady state with total power averaging around the expected 1.35 kW level.

The time evolution of the discharge current can be further analyzed by plotting spectrogram of the power spectrum, as shown in Fig. 3. These plots were created with a Python script that parses the HPHall output log file and uses the built-in FFT routines to compute the spectrum along a sliding window covering 5000 1×10^{-7} time steps. The contour values correspond to $10 \log_{10}(P_s/\max(P_s))$. Time increases from the bottom to the top. The initial current spike can be seen along the bottom edge as higher power across a wideband of frequencies. The thruster quickly achieves an oscillatory steady state with dominant modes at 15 and 90 kHz.

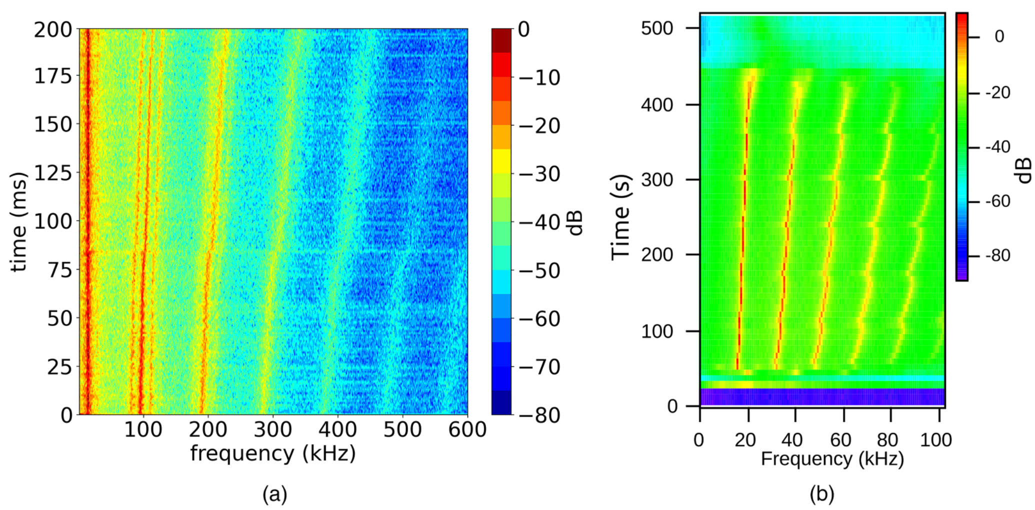

FIG. 5. (a) Numerical discharge frequency spectrum for a linear 10^{-4} Torr/s pressure increase and (b) experimentally observed spectrum during thruster startup reproduced from W. A. Hargus and B. Pote, "Examination of a Hall thruster start transient," in *38th AIAA/ASME/SAE/ASEE Joint Propulsion Conference & Exhibit* (AIAA, 2002).[37]

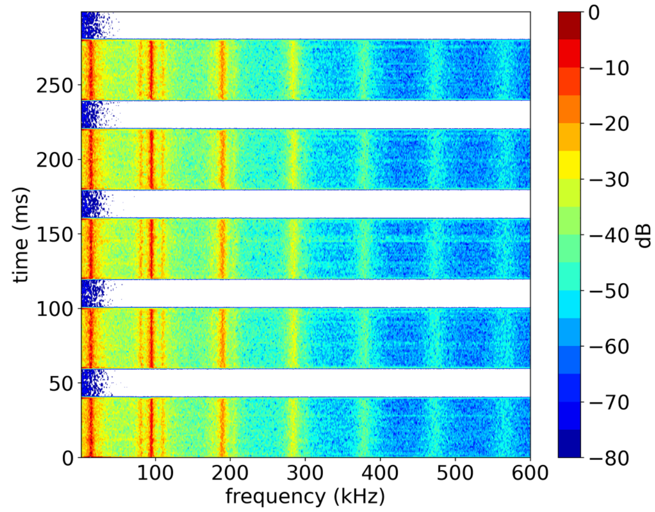

FIG. 6. Frequency spectrum from a quasi-steady operation.

B. Uniform pressure increase

Next, we considered the response of the simulated thruster to a variation in chamber pressure. The goal of this study was to verify that the background neutral injection model described in Sec. III A does indeed affect the thruster behavior. Here we utilized the constant dp/dt model, with pressure increasing linearly from 10^{-6} Torr. We ran several simulations with the pressure rate of increase ranging from 10^{-4} Torr/s to upward of 10^{-2} Torr/s. The plot in Fig. 4 corresponds to this latter rate, while the inset illustrates the increase at a slower 10^{-3} Torr/s. The slower rate of increase allowed us to capture additional detail in the numerical results, since data are exported at a fixed time step frequency. The plot shown in the inset thus effectively increases the detail in the main figure over the selected pressure range.

A pressure response is clearly visible in the inset plot of Fig. 4. High-frequency modes become quenched as the pressure grows, and at approximately 1.5×10^{-4} Torr, only the primary breathing mode remains, along with a broad signal extending to 200 kHz. The amplitude of the breathing mode grows with an increase in pressure, along with a new 100 kHz mode that appears at approximately 1.1×10^{-3} Torr. These modes continue growing in amplitude as the ambient neutrals provide the thruster with an additional source of propellant. In a real device, this growth in discharge oscillations would likely lead to testing difficulties and an eventual thruster failure.

Figure 5(a) zooms further on the power spectrum variation at the start of the simulation by considering a run with $dp/dt = 10^{-4}$ Torr/s. We can clearly observe a nearly linear drift of the dominant frequencies as the pressure increases, with the drift rate increasing at higher frequencies. Interestingly, a similar drift in the frequency space was observed experimentally by Hargus *et al.*[37] utilizing a different thruster, Fig. 5(b). It was speculated to correspond to a pressure increase from outgassing. Since the outgassing rate is proportional to surface temperature, it is reasonable to expect the contaminant pressure to increase as the thruster warms up. Our forced pressure increase can be expected to have a similar effect on the thruster behavior.

C. Quasi-steady operation

The original goal of this work was to scale the SPT-100 thruster simulation to the >100 kW range following the scaling model of Misuri.[49] However, challenges were encountered along the way, possibly involving a need to increase the computational mesh refinement while no longer having access to the mesh generator. Instead, we simulate the baseline 1.35 kW SPT-100 operating in a small chamber of a reduced pumping speed. Equation (6) indicates that pumping speed and chamber volume can be scaled by the factor $1.35/P_t$ to retain the pressure increase of a thruster operating at P_t kW power. Using this ratio, the pressure increase of the 1.35 kW device can be made comparable to a high-power thruster operating in a larger chamber. The simulation was scaled to approximate a 1 MW class device operating in the same facility used in Fig. 1. Flow control was adjusted to consist of a 40 ms nominal operation followed by a 20 ms low flow case, in which the mass flow rate was reduced by a factor of 10. Given that HPHall is not parallelized, it takes the code almost a day to simulate just 0.01 s of real time, and the pulse sequence described here required almost 3 weeks of run time. In the experimental testing, the pulse duration would be selected based on the rate of pressure increase for a given chamber and pump configuration. For the conditions described in Fig. 1, the pulse duration could be extended to over 1 s for a 100 kW class device.

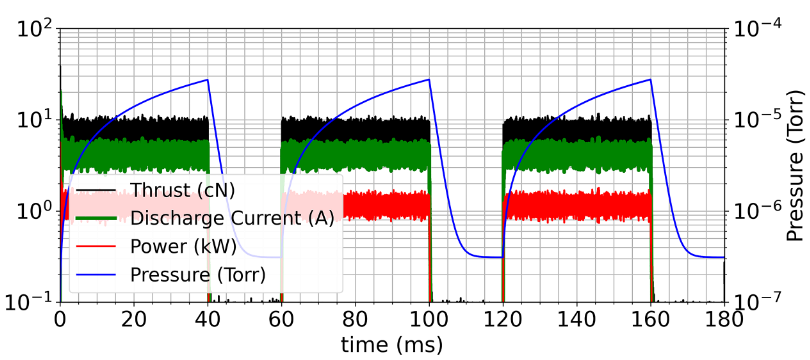

FIG. 7. Temporal variation in T, I_d, P, and p.

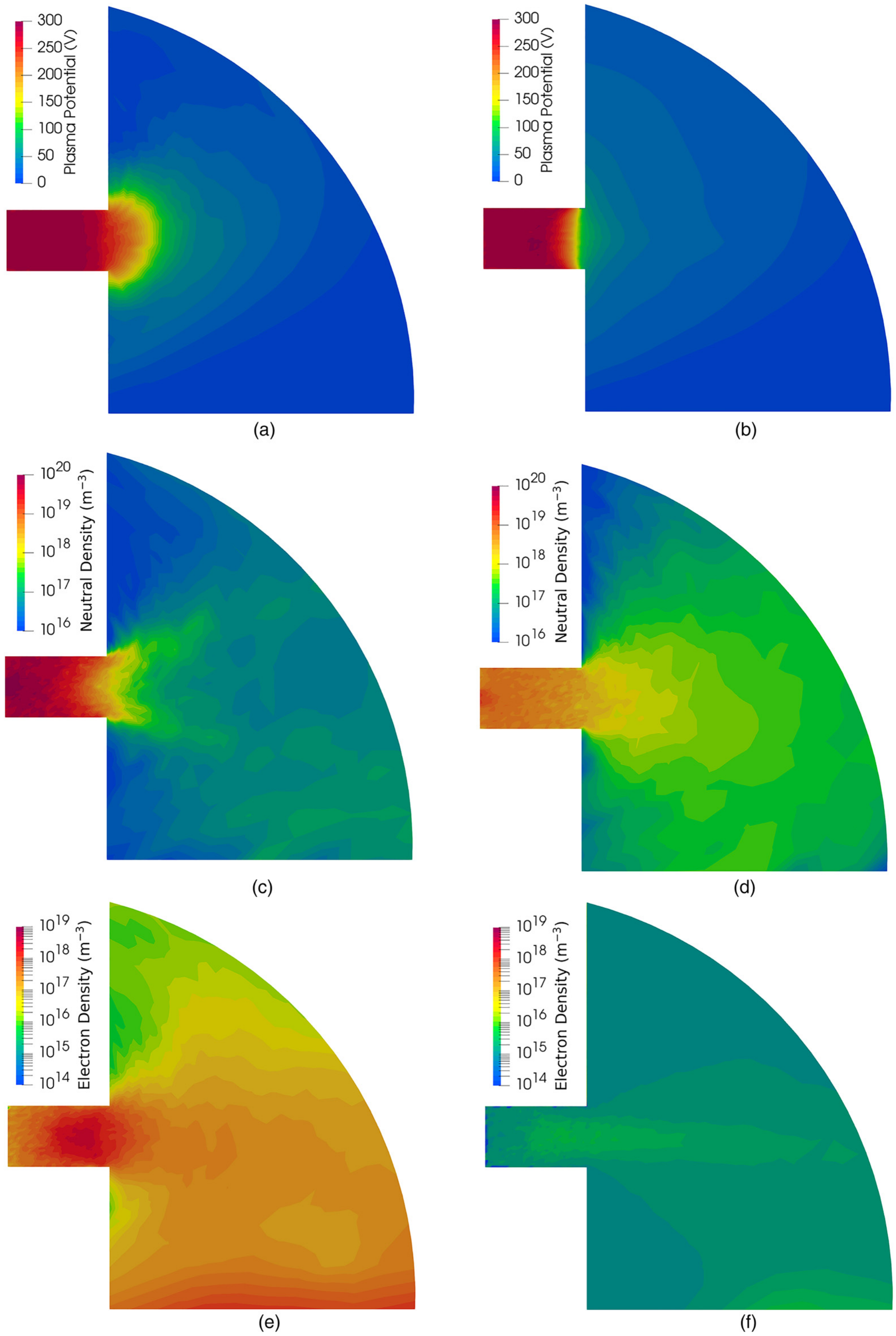

FIG. 8. Typical simulated (a) and (b) plasma potential, (c) and (d) neutral density, and (e) and (f) electron density for the nominal and low flow mode.

Figure 6 plots the frequency spectrum from the quasi-steady operation. Good agreement can be seen by comparison with Fig. 3. We do not observe any noticeable impact of the background pressure on the power spectrum. This finding is expected, since each pulse terminated before the facility pressure had a chance to increase above 3×10^{-5} Torr. The corresponding thrust, discharge current, power, and chamber pressure are shown in Fig. 7. We can observe an excellent repeatability between cycles and with the steady-state nominal operation in Fig. 2. The gaps can be easily removed in post-processing, leaving us with a continuous trace of discharge current. Near-plume plasma potential and current density measurements can be used to estimate thrust if a thrust stand settling time proves to be incompatible with the pulse duration.[50] Characterization of repeatability in the laboratory setting is planned as future work.

The variation in the mesh-averaged simulation results computed by HPHall for the nominal and low flow cycles is shown in Fig. 8. We can see that in the low flow mode phase, the potential profile corresponds to an almost linearly decaying drop from the anode to the cathode potential. In the nominal mode, Fig. 8(a), the acceleration zone is pushed outward. Plots 8(c) and 8(d) compare the neutral density. While the density in the channel decreases in the low flow mode, as expected, the neutral density downstream of the exit plane is actually increased in this mode due to the reduced loss of neutrals to ionization. The final set of plots compares the electron density, which per quasineutrality balances the total ion charge density. It is reduced by almost 3 orders of magnitude.

V. LIFETIME TESTING AND SECONDARY EFFECTS

While quasi-steady operation appears to be an attractive method for characterizing performance and plume characteristics of high-power Hall thrusters using facilities with limited pumping. However, the major challenge remains in lifetime testing. Utilizing the simple model visualized in Fig. 1, the chamber requires approximately 40 s to reduce the pressure to the baseline following each pulse. Assuming a 1 s measurement time available at 100 kW, this difference between testing and pump down times implies a 40 × increase in lifetime testing time line. This time line could be decreased by delegating aspects of lifetime characterization to the numerical analysis and using acceleration techniques such as a careful removal of the discharge channel material following the predicted erosion pattern.

Furthermore, there is some evidence of second-order hardware temperature effects influencing HET performance and lifetime. One way to incorporate these effects is to operate a high-power thruster for a period of hours at a poor facility pressure until the hardware temperature reaches the steady state. The thruster performance and lifetime measurements would be uncertain for this phase, but the hardware temperature distribution should not be strongly affected by the background pressure if the desired power level is maintained.

The anode flow would then be reduced to reduce the chamber pressure, while maintaining the cathode flow to keep the cathode hot. If the thruster cools slowly and nearly maintains its steady-state temperature distribution, this approach will allow us to reproduce a near-steady-state temperature profile, a good space-like vacuum, and critical thruster and plume measurements with correct distributions.

VI. CONCLUSION

While having been identified as enabling technologies for a range of new space missions, the development of high-power Hall thruster remains hindered by the low number of facilities available for testing in the 100 kW range and *no* facilities for testing at MW power levels. In this article, we identified a testing approach for high power Hall thrusters based on quasi-steady pulsed operation. We propose to run the device in a series of pulses during which the propellant flow rate is cycled between the nominal and a reduced value to allow the chamber pressure to recover. The thruster remains powered in the low flow mode to reduce electrical transient effects encountered with restarts. We utilize a numerical simulation to demonstrate that the pulsed operation is able to reproduce characteristic properties such as the discharge current spectrum in the time interval until the chamber pressure exceeds a critical background pressure. We also visualized the predicted near plume plasma profiles for the nominal and low configuration and discussed implications for lifetime testing.

ACKNOWLEDGMENTS

This research was partially funded through AFOSR Grant No. FA9550-19-1-0166.

VII. AUTHOR DECLARATIONS

A. Conflict of Interest

The authors have no conflicts to disclose.

DATA AVAILABILITY

The data that support the findings of this study are available from the corresponding author on request. Scripts used for generation of plots of pressure evolution (Fig. 1), HPHall performance metrics (Fig. 2), and frequency spectrum (Fig. 3 and similar) are available in Quasi Steady-State Testing Approach for Hall Thrusters at https://www.particleincell.com/2021/qs-het, Ref. 51.

REFERENCES

[1]W. Andrew Hoskins, R. Joseph Cassady, O. Morgan, R. Myers, F. Wilson, D. Q. King, and K. deGrys, "30 years of electric propulsion flight experience at aerojet rocketdyne," in *33rd International Electric Propulsion Conference, Washington, DC* (Electric Rocket Propulsion Society, 2013), pp. 1–12, IEPC-2013-439.

[2]J. Jackson, S. Miller, J. Cassady, E. Soendker, B. Welander, M. Barber, and P. Peterson, "13 kw advanced electric propulsion flight system development and qualification," in *36th International Electric Propulsion Conference, Vienna* (Electric Rocket Propulsion Society, 2019).

[3]D. Manzella, R. Jankovsky, and R. Hofer, "Laboratory model 50 kw Hall thruster," in *38th AIAA/ASME/SAE/ASEE Joint Propulsion Conference & Exhibit* (AIAA, 2002), p. 3676.

[4]D. Jacobson and D. Manzella, "50 kw class krypton Hall thruster performance," in *39th AIAA/ASME/SAE/ASEE Joint Propulsion Conference and Exhibit* (AIAA, 2003), p. 4550.

[5]S. J. Hall, B. J. Jorns, A. D. Gallimore, H. Kamhawi, T. W. Haag, J. A. Mackey, J. H. Gilland, P. Y. Peterson, and M. Baird, "High-power performance of a 100-

kW class nested Hall thruster," paper presented at the 35th International Electric Propulsion Conference (IEPC), Atlanta, GA, 8–12 October 2017.
[6]R. Florenz, T. Liu, A. Gallimore, H. Kamhawi, D. Brown, R. Hofer, and J. Polk, "Electric propulsion of a different class: The challenges of testing for megawatt missions," in *48th AIAA/ASME/SAE/ASEE Joint Propulsion Conference & Exhibit* (AIAA, 2012).
[7]S. E. Cusson, M. P. Georgin, H. C. Dragnea, E. T. Dale, V. Dhaliwal, I. D. Boyd, and A. D. Gallimore, "On channel interactions in nested Hall thrusters," J. Appl. Phys. **123**(13), 133303 (2018).
[8]R. Spores, J. Monheiser, B. P. Dempsey, D. Wade, K. Creel, D. Jacobson, and G. Drummond, "A solar electric propulsion cargo vehicle to support NASA lunar exploration program," in *IEPC Paper No. IEPC-2005-320, 25th International Electric Propulsion Conference, Princeton, NJ, October* (Electric Rocket Propulsion Society, 2005), Vol. 31.
[9]N. Strange, R. Merrill, D. Landau, B. Drake, J. Brophy, and R. Hofer, "Human missions to phobos and deimos using combined chemical and solar electric propulsion," in *47th AIAA/ASME/SAE/ASEE Joint Propulsion Conference & Exhibit* (AIAA, 2011), p. 5663.
[10]R. Florenz, A. D. Gallimore, and P. Y. Peterson, "Developmental status of a 100-kw class laboratory nested channel Hall thruster," in *32nd International Electric Propulsion Conference (IEPC), Wiesbaden* (Electric Rocket Propulsion Society, 2011), pp. 1–9.
[11]J. D. Frieman, J. A. Walker, M. L. R. Walker, V. Khayms, and D. Q. King, "Electrical facility effects on Hall thruster cathode coupling: Performance and plume properties," J. Propul. Power **32**(1), 251–264 (2016).
[12]J. A. Walker, J. D. Frieman, M. L. R. Walker, V. Khayms, D. King, and P. Y. Peterson, "Electrical facility effects on Hall-effect-thruster cathode coupling: Discharge oscillations and facility coupling," J. Propul. Power **32**(4), 844–855 (2016).
[13]J. D. Frieman, T. M. Liu, and M. L. R. Walker, "Background flow model of Hall thruster neutral ingestion," J. Propul. Power **33**(5), 1087–1101 (2017).
[14]W. G. Tighe, R. Spektor, K. Diamant, and H. Kamhawi, "Effects of background pressure on the NASA 173 m Hall current thruster performance," in *34th International Electric Propulsion Conference* (Electric Rocket Propulsion Society, 2015).
[15]B. M. Reid, "Empirically-derived corrections for facility effects in performance and plume measurements of Hall thrusters," in *34th International Electric Propulsion Conference* (Electric Rocket Propulsion Society, 2015).
[16]R. R. Hofer and J. R. Anderson, "Finite pressure effects in magnetically shielded Hall thrusters," in *50th AIAA/ASME/SAE/ASEE Joint Propulsion Conference* (AIAA, 2014), p. 3709.
[17]Y. Raitses, J. Parker, E. Davis, and N. Fisch, "Background gas pressure effects in the cylindrical Hall thruster," in *46th AIAA/ASME/SAE/ASEE Joint Propulsion Conference & Exhibit* (AIAA, 2010), p. 6775.
[18]T. S. Matlock, M. R. Nakles, and R. Spektor, "Pressure dependence of near-field plume properties in a 1 kw laboratory Hall thruster," in *35th International Electric Propulsion Conference* (Electric Rocket Propulsion Society, 2017).
[19]T. Randolph, V. Kim, H. Kaufman, K. Kozubsky, V. V. Zhurin, and M. Day, "Facility effects on stationary plasma thruster testing," in *23rd International Electric Propulsion Conference* (Electric Rocket Propulsion Society, 1993), pp. 13–16.
[20]J. Steven Snyder, G. Lenguito, J. D. Frieman, T. W. Haag, and J. A. Mackey, "Effects of background pressure on spt-140 Hall thruster performance," J. Propul. Power **36**(5), 668–676 (2020).
[21]M. P. Byrne, B. A. Jorns, and A. Arbor, "Data-driven models for the effects of background pressure on the operation of Hall thrusters," in *36th International Electric Propulsion Conference (IEPC), Vienna* (Electric Rocket Propulsion Society, 2019), pp. 15–20.
[22]J. S. Sovey, R. H. Vetrone, S. P. Grisnik, R. M. Myers, and J. E. Parkes, "Test facilities for high-power electric propulsion," J. Propul. Power **10**(1), 18–24 (1994).
[23]W. A. Rodriguez and J. Dankanich, "National space simulation facility concept design," in *35th International Electric Propulsion Conference, IEPC-2017-16* (Electric Rocket Propulsion Society, Atlanta, GA, 2017).
[24]J. T. Yim, D. A. Herman, and J. M. Burt, "Modeling analysis for NASA GRC vacuum facility 5 upgrade," Technical report NASA/TM–2013-216496 (National Aeronautics and Space Administration, Glenn Research Center, 2013).
[25]D. Schoeffler and M. W. Crofton, "Design of electric propulsion testing facility with custom cryopumping system," in *AIAA Scitech 2019 Forum* (AIAA, 2019), p. 1244.
[26]J. D. Frieman, H. Kamhawi, P. Y. Peterson, D. A. Herman, J. H. Gilland, and R. R. Hofer, "Completion of the long duration wear test of the NASA HERMeS Hall thruster," in *AIAA Propulsion and Energy 2019 Forum* (AIAA, 2019), p. 3895.
[27]A. Kieckhafer and L. B. King, "Energetics of propellant options for high-power Hall thrusters," J. Propul. Power **23**(1), 21–26 (2007).
[28]K. E. Clark and R. G. Jahn, "Quasi-steady plasma acceleration," AIAA J. **8**(2), 216–220 (1970).
[29]E. Choueiri and J. Ziemer, "Quasi-steady magnetoplasmadynamic thruster measured performance database," J. Propul. Power **17**(5), 967–976 (2001).
[30]M. LaPointe and P. Mikellides, "High power MPD thruster development at the NASA Glenn Research Center," in *37th Joint Propulsion Conference and Exhibit* (AIAA, 2001), p. 3499.
[31]V. Hruby, B. Pote, M. Gamero-Castano, R. Tedrake George Kolencik, L. Byrne, and M. Delichatsios, "Hall thrusters operating in pulsed mode," in *27th International Electric Propulsion Conference, Pasadenca, CA* (Electric Rocket Propulsion Society, 2001).
[32]V. J. Hruby, B. M. Pote, and M. Gamero-Castano, "Pulsed Hall thruster system," U.S. patent 6,735,935 (18 May 2004).
[33]J. M. Fife, "Hybrid-PIC modeling and electrostatic probe survey of Hall thrusters," Ph.D thesis (Massachusetts Institute of Technology, 1998).
[34]M. Sekerak, M. McDonald, R. Hofer, and A. Gallimore, "Hall thruster plume measurements from high-speed dual langmuir probes with ion saturation reference," in *2013 IEEE Aerospace Conference* (IEEE, 2013).
[35]R. Bryant Lobbia, "A time-resolved investigation of the Hall thruster breathing mode," Ph.D thesis (University of Michigan, 2010).
[36]D. Guo, M. Cheng, and X. Li, "Design and test of a simple fast electromagnetic inductive gas valve for planar pulsed inductive plasma thruster," Rev. Sci. Instrum. **88**(10), 105101 (2017).
[37]W. A. Hargus and B. Pote, "Examination of a Hall thruster start transient," in *38th AIAA/ASME/SAE/ASEE Joint Propulsion Conference & Exhibit* (AIAA, 2002), p. 3956.
[38]W. A. Hargus, "Investigations of an environmentally induced long duration Hall thruster start transient," Technical report (Air Force Research Lab, Propulsion Directorate, Edwards AFB, 2006).
[39]R. Santos, E. Ahedo, Y. Raitses, and N. J. Fisch, "Transitional regime in the start-up process of conventional Hall thrusters," in *32nd International Electric Propulsion Conference (IEPC)* (Electric Rocket Propulsion Society, 2011).
[40]C. L. Ellison, Y. Raitses, and N. J. Fisch, "Fast camera imaging of Hall thruster ignition," IEEE Trans. Plasma Sci. **39**(11), 2950–2951 (2011).
[41]S. Yan, W. Li, Y. Ding, L. Wei, and D. Yu, "High-speed camera imaging in the discharge channel during a Hall thruster ignition," IEEE Trans. Plasma Sci. **46**(4), 1058–1061 (2018).
[42]ICARE, see https://youtu.be/hTlcYbIrgmQ?t=43 for "ISCT-100 - ICARE's Hall thruster demonstration" (accessed July 2021).
[43]See https://news.satnews.com/2021/03/31/solar-electricpropulsionsystemhot-firetesting-completed-by-maxar-busek/ for "SatNews: Solar electric propulsion system hot fire testing completed by maxar + busek" (accessed July 2021).
[44]S. Y. Cheng and M. Martinez-Sanchez, "Hybrid particle-in-cell erosion modeling of two Hall thrusters," J. Propul. Power **24**(25), 987–998 (2008).
[45]R. R. Hofer, I. G. Mikellides, I. Katz, and D. M. Goebel, "Wall sheath and electron mobility modeling in hybrid-PIC Hall thruster simulations," in *43rd AIAA/ASME/SAE/ASEE Joint Propulsion Conference & Exhibit, Cincinnati, OH* (AIAA, 2007).
[46]F. I. Parra, D. Escobar, and E. Ahedo, "Improvements on particle accuracy in a Hall thruster hybrid code," in *42nd AIAA/ASME/SAE/ASEE Joint Propulsion Conference & Exhibit, Sacrament, CA* (AIAA, 2006).
[47]R. Santos and E. Ahedo, "Accuracy improvements in a Hall thruster PIC/fluid code," in *45th AIAA/ASME/SAE/ASEE Joint Propulsion Conference & Exhibit, Denver, CO* (AIAA, 2009).

[48]L. Brieda, J. Koo, and M. Scharfe, "Influence of a power supply model on simulated Hall thruster discharge voltage oscillations," AIP Adv. **9**(2), 025320 (2019).
[49]T. Misuri, F. Battista, C. Barbieri, E. Alessio De Marco, and M. Andrenucci, "High power Hall thruster design options," in *Proceedings of the 30th International Electric Propulsion Conference (Florence), IEPC* (Electric Rocket Propulsion Society, 2007).
[50]T. Zhuang, A. Shashurin, T. Denz, M. Keidar, P. Vail, and A. Pancotti, "Performance characteristics of micro-cathode ARC thruster," J. Propul. Power **30**(1), 29–34 (2014).
[51]See https://www.particleincell.com/2021/qs-het for information about the quasi steady-state testing approach for Hall thrusters, with links to download the codes.